

Thermal convection thresholds in a Oldroyd magnetic fluid

L.M. Pérez^a, J. Bragard^b, D. Laroze^{*,c,d}, J. Martinez-Mardones^e, H. Pleiner^c

^aDepartamento de Ingeniería Metalúrgica, Universidad de Santiago de Chile, Av. Bernardo OHiggins 3363, Santiago, Chile.

^bDepartamento de Física y Matemática Aplicada, Universidad de Navarra, 31080 Pamplona, Spain

^cMax Planck Institute for Polymer Research, D 55021 Mainz, Germany

^dInstituto de Alta Investigación, Universidad de Tarapacá, Casilla 7D, Arica, Chile

^eInstituto de Física, Pontificia Universidad Católica de Valparaíso, Casilla 4059, Valparaíso, Chile

Abstract

We report theoretical and numerical results on convection for a magnetic fluid in a viscoelastic carrier liquid. The viscoelastic properties is given by the Oldroyd model. We obtain explicit expressions for the convective thresholds in terms of the parameters of the system in the case of idealized boundary conditions. We also calculate numerically the convective thresholds for the case of realistic boundary conditions. The effect of the Kelvin force and of the rheology on instability thresholds for a diluted suspensions are emphasized.

Key words: Thermal convection, magnetic fluid, viscoelastic fluid.

1. Introduction

Ferrofluids are magnetic fluids formed by a stable colloidal suspension of magnetic nanoparticles dispersed in a carrier liquid. Without an applied external magnetic field the orientations of the magnetic moments of the particles are random resulting in a vanishing macroscopic magnetization (magnetic disorder). An external magnetic field, however, easily orients the particle magnetic moments and a large (induced) magnetization is obtained. There are two main features that distinguish ferrofluids from ordinary fluids, the polarization force and the body couple. In the last decades much efforts have been dedicated to the study the phenomenon of convective mechanism in ferrofluids. In addition, heat transfer through magnetic fluids, in particular, have been one of the leading area of scientific study due to its technological applications [1]. The ferrofluid convection has application in high-power capacity transformer system where the ferrofluid is used as a material in the core as well as a coolant in the transformer. To activate convective cooling, knowledge of concentration gradient, which will induce convection, is required. An important application of ferrofluids lies in the biomedicine area where the carrier liquid is blood [2, 3, 4, 5, 6] which is known to have also special rheological proprieties [7, 8, 9]. In addition, when a magnetic field is applied, the ferrofluid can exhibit additional rheological properties such as magneto-viscosity, adhesion properties, non-Newtonian behavior, among others [10, 11, 12, 13, 14, 15, 16, 17, 18, 19, 20]. Hence, a detailed study of viscoelastic magnetic fluids is quite important and in order.

The first continuum description of magnetic fluids was given by Neuringer and Rosensweig [21]. Later, Finlayson [22] studied the convective instability of a magnetic fluid for a fluid layer heated from below in the presence of a uniform vertical magnetic field. He discussed the cases of both, shear free and rigid horizontal boundaries using the linear stability method. Gotoh and Yamada [23] carried out a similar study by assuming the fluid to be confined between two magnetic pole pieces. A weakly nonlinear analysis in a strong external field was considered by Blennerhassett et al. [24]. The convective instability for a rotating layer in a magnetic fluid has been studied by Gupta and Gupta [25] and by Venkatasubramanian and Kaloni [26]. An amplitude equation for the stationary convection with idealized boundary condition was derived in Ref.[27]. The Küppers-Lortz instability for the case of a rotating magnetic fluid was formulated by Auernhammer and Brand [28]. Ryskin and Pleiner [29], using nonequilibrium thermodynamics, have derived a complete set of equations to describe ferrofluids in an external magnetic field. This description is made in terms of a binary mixture, where the magnetophoretic effect, as well as magnetic stresses, have been taken into account in the static and dynamic parts of the ferrofluid equations. When the magnetophoretic effect can be neglected, we have analyzed the thermal convection for rotating ferrofluids. For idealized boundary condition for the typical conductive state in the stationary case an analytical expression was found for the Rayleigh number as function of control parameters [30]. Recently, the weakly nonlinear analysis for stationary convection in a rotating magnetic binary mixture was studied [31]. Other effects, such as the buoyancy-surface tension effects, nonuniform thermal gradients, magnetization constitutive equations, etc., have also been studied in Refs. [32, 33, 34, 35, 36, 37, 38].

Viscoelastic properties of fluids can be described by a constitutive equation, which relates the stress and strain rate ten-

*Corresponding author at: Max Planck Institute for Polymer Research, D 55218 Mainz, Germany

Email address: david.laroze@gmail.com (D. Laroze)

sors. Finding this relation, which should generalize the linear dependence characteristic of Newtonian fluids, is the main purpose of the science of Rheology. The simplest constitutive equation capable of describing realistically the viscoelastic properties is given by the so-called Oldroyd model [39]. In this model, the stress tensor is decomposed into both a polymeric contribution and a solvent contribution. Studies of convection in such fluids have been performed by various authors for different cases, either with free-free or rigid-rigid boundary conditions [40, 41, 43, 44, 45, 46, 47, 42, 48, 49, 50, 51, 52, 53, 54, 55]. It has been found that, besides the usual stationary convection, oscillatory states can also be obtained at onset. Which type of convection - stationary or oscillatory appears - first will depend on the values of the rheological parameters. Experimental measurements of oscillatory convection in viscoelastic mixtures were reported by Kolodner [56] in a DNA suspension; and theoretical studies of the convection thresholds for binary viscoelastic mixtures in different types of fluids, can be found in Refs. [57, 58, 59, 60, 61]. Recently, studies on stationary convection in viscoelastic magnetic fluid have been done [62, 63].

The purpose of the present paper is to analyze the influence of the viscoelasticity in convective thresholds in magnetic fluid, in particular, where the separation ratio and magnetic separation ratio are not too large the simple fluid approximation can be used [29]. To this aim an Oldroyd viscoelastic magnetic fluids heated from below is considered. The description of the system involves many parameters whose values have not yet been determined accurately. Therefore, we are left with some freedom in fixing the parameter values. In order to be as exhaustive as possible, we will analyze the linear regime for two different limiting cases of boundary condition i.e. the free-free (FF) and the rigid-rigid (RR) boundary conditions. In the first case (FF), one can explicitly calculate the threshold for convection in function of the parameters of the fluid. In addition, we have further checked that we retrieved the previous results obtained in simplified situations by other authors. In the case of realistic boundary conditions (RR), an analytical calculation is not tractable and we numerically solve the linearized system using a collocation spectral method in order to determine the eigenfunctions and eigenvalues and consequently the convective thresholds. The paper is organized as follows: In Sec. 2, the basic hydrodynamic equations for viscoelastic magnetic fluid convection are presented. In Sec. 3 the linear stability analysis of the conduction state is performed. Finally, conclusions are presented in Sec. 4.

2. Basic Equations

We consider a layer of incompressible magnetic fluid in a viscoelastic carrier liquid, of thickness d , parallel to the xy -plane, with very large horizontal extension in a gravitational field \mathbf{g} and subject to a vertical temperature gradient. The magnetic fluid properties can be modeled as electrically nonconducting superparamagnets. The magnetic field \mathbf{H} is assumed to be oriented in a direction parallel to the \hat{z} axis. It would be homogeneous, if the magnetic fluid were absent. Let us choose the z -axis such that $\mathbf{g} = -g\hat{z}$ and that the layer has its interfaces at

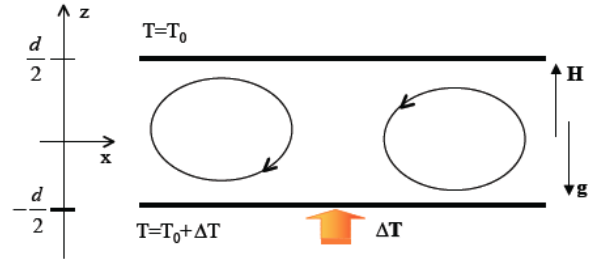


Figure 1: A vertical cut through the fluid layer. Note the y -axis point into the xz -plane.

coordinates $z = -d/2$ and $z = d/2$. A static temperature difference across the layer is imposed, $T(z = -d/2) = T_0 + \Delta T$ and $T(z = d/2) = T_0$. The set-up of the problem is drawn in Fig. 1. Under the Boussinesq approximation, the balance equations read as

$$\nabla \cdot \mathbf{v} = 0, \quad (1)$$

$$\rho_0 d_t \mathbf{v} = -\nabla p_{eff} + \nabla \cdot \bar{\boldsymbol{\tau}} + \rho \mathbf{g} + \mathbf{M} \cdot \nabla \mathbf{H}, \quad (2)$$

$$\frac{c_{v,\mathbf{H}}}{T_0} d_t T + \chi_T \mathbf{H}_0 \cdot d_t \mathbf{H} = \bar{\kappa} \nabla^2 T + \vartheta \mathbf{H}_0 \cdot \nabla^2 \mathbf{H}, \quad (3)$$

where $d_t f = \partial_t f + \mathbf{v} \cdot \nabla f$ is the total derivative, \mathbf{v} is the velocity field, p_{eff} is the effective pressure which contains the static hydrodynamic pressure and the gradient term of the magnetic force, ρ is the mass density, ρ_0 is a reference mass density, $\bar{\boldsymbol{\tau}}$ is the extra stress tensor, \mathbf{M} is the magnetization field, $c_{v,\mathbf{H}}$ is the specific heat capacity at constant volume and magnetic field, T is the temperature, T_0 is a reference temperature, χ_T is the pyromagnetic coefficient and $\bar{\kappa}$ is the thermal diffusivity, and $\vartheta \propto \chi_H / \rho_0$, being χ_H the magnetic susceptibility along the field.

For the total density we use the following linear state equation

$$\rho = \rho_0 (1 - \alpha_T \Delta T + \alpha_H \mathbf{H}_0 \cdot \Delta \mathbf{H}) \quad (4)$$

where α_T and α_H are the thermal and the magnetic expansion coefficients, respectively. In the following, we denote $\Delta f = f - f_0$. In addition, for the magnetic field \mathbf{H} and the magnetic induction \mathbf{B} , we suppose that the system is not conductive, i.e., it is governed by Maxwell equations

$$\nabla \times \mathbf{H} = \mathbf{0}, \quad (5)$$

$$\nabla \cdot \mathbf{B} = 0. \quad (6)$$

Furthermore, we assume a linear relationship between these fields $\mathbf{B} = \mathbf{H} + \mathbf{M}$ and introduce the scalar magnetic potential $\mathbf{H} = -\nabla \phi$ to fulfill Eq. (5). The magnetization field is assumed to follow instantaneously the external field $\mathbf{M} = M(T, H) \hat{\mathbf{H}}$ with the usual phenomenological equation of state

$$M(T, H) = M_0 - \chi_T \Delta T + \chi_H \mathbf{H}_0 \cdot \Delta \mathbf{H} \quad (7)$$

where Δ denotes deviations from the ground state.

A constitutive equation relating the extra stress tensor $\bar{\boldsymbol{\tau}}$ and the shear rate has also to be introduced. In a Newtonian incompressible fluid, the extra stress tensor is related to the strain tensor via the Newton law, $\bar{\boldsymbol{\tau}} = 2\nu\bar{\mathbf{D}}$, where $\bar{\mathbf{D}}$ is the symmetric part of the velocity field gradient and ν is the kinematic viscosity. For complex polymeric fluids, a more general constitutive relation between stress and strain rate $\bar{\boldsymbol{\tau}} = \bar{\boldsymbol{\tau}}(\bar{\mathbf{D}})$ is necessary to describe the behavior. This last relation is subjected to symmetry restrictions. One type of constitutive relation that satisfies these symmetry requirements and that may be further justified by the kinetic theory of dumbbells has been proposed by Oldroyd [39]. This family of models, developed in the fifties of the last century, include particular cases that are widely used for different kinds of polymeric solutions. In the Oldroyd model, the constitutive equation is written as

$$(1 + \lambda_1 D_t)\bar{\boldsymbol{\tau}} = 2\nu(1 + \lambda_2 D_t)\bar{\mathbf{D}}, \quad (8)$$

where ν is the static viscosity, λ_1 is the relaxation time, and λ_2 is the retardation time, the last two parameters characterize the viscoelastic time scales. For thermodynamic stability reasons both, λ_1 and λ_2 , are taken to be positive. The symbol D_t in Eq. (8) denotes an invariant ("frame-indifferent") time derivative, defined as

$$D_t\bar{\boldsymbol{\tau}} = d_t\bar{\boldsymbol{\tau}} + \bar{\boldsymbol{\tau}} \cdot \bar{\mathbf{W}} - \bar{\mathbf{W}} \cdot \bar{\boldsymbol{\tau}} + a(\bar{\boldsymbol{\tau}} \cdot \bar{\mathbf{D}} + \bar{\mathbf{D}} \cdot \bar{\boldsymbol{\tau}}), \quad (9)$$

where $\bar{\mathbf{W}}$ is the skew-symmetric part of the velocity field gradient; also a is a phenomenological parameter that lies in the range -1 to $+1$. For $a = -1$, one gets the lower convected Jeffrey's model (Oldroyd B), for $a = 0$ one gets the so-called corotational Jeffrey's model, and $a = 1$ describes the upper convected Jeffrey's model (Oldroyd A). Let us comment that the coefficient a is not completely independent of the other rheological parameters [68]. Some limiting cases are $\lambda_2 = 0$ that leads to a Maxwellian fluid, while a Newtonian fluid requires both $\lambda_1 = 0$ and $\lambda_2 = 0$.

Let us now analyze the boundary conditions (BCs) of the system. A static temperature difference across the layer is imposed, $T(z = -d/2) = T_0 + \Delta T$ and $T(z = d/2) = T_0$; as the magnetic BCs we use the typical continuity conditions of the Maxwell equations, i.e., $\mathbf{n} \times (\mathbf{H}_{in} - \mathbf{H}_{ex}) = \mathbf{0}$ and $\mathbf{n} \cdot (\mathbf{B}_{in} - \mathbf{B}_{ex}) = 0$, where \mathbf{n} is a unit vector normal to the boundaries. Moreover, for the velocity field we will consider both Free-Free (FF) and Rigid-Rigid (RR) interfaces. Hence, from Eqs. (1)–(8) and using these boundary conditions the conductive basic rest state is given by

$$\mathbf{v}_{con} = \mathbf{0}, \quad (10)$$

$$T_{con}(z) = \bar{T} - \beta z, \quad (11)$$

$$\mathbf{H}_{con}(z) = \mathbf{H}_0(1 + \lambda\beta z), \quad (12)$$

where $\beta = (\Delta T/d)$ and $\lambda = \chi_T/(1 + \chi_H)$. After some algebra, the equations for the dimensionless perturbations can be written as

$$\nabla \cdot \mathbf{v} = \mathbf{0} \quad (13)$$

$$P^{-1}d_t\mathbf{v} = -\nabla p_{eff} + \nabla \cdot \bar{\boldsymbol{\tau}} + Ra\boldsymbol{\Sigma} \quad (14)$$

$$(1 + \Gamma D_t)\bar{\boldsymbol{\tau}} = (1 + \Gamma\Lambda D_t)\bar{\mathbf{D}} \quad (15)$$

$$d_t(\theta - M_4\partial_z\phi) = (1 - M_4)w + \nabla^2\theta \quad (16)$$

$$(\partial_{zz} + M_3\nabla_{\perp}^2)\phi - \partial_z\theta = 0 \quad (17)$$

$$\nabla^2\phi_{ext} = 0 \quad (18)$$

where $\{v, \theta, \phi\}$ are the dimensionless velocity perturbation, the temperature perturbation and the dimensionless magnetic potential perturbation, respectively; and where $\boldsymbol{\Sigma} = \Pi_1(\theta, \phi)\hat{\mathbf{z}} + M_1\theta\nabla(\partial_z\phi)$ with $\Pi_1 = (1 + M_1)\theta - (M_1 - M_5)\partial_z\phi$ and $\nabla_{\perp}^2 = \partial_{xx} + \partial_{yy}$. In Eqs. (13)–(18), the following groups of dimensionless numbers have also been introduced: **(a)** (pure fluids) The Rayleigh number, $Ra = \alpha_T g \Delta T d^3 / \kappa \nu$, accounting for buoyancy effects; and the Prandtl number, $P = \nu / \kappa$, relating viscous and thermal diffusion time scales. **(b)** (magnetic fluid) The strength of the magnetic force relative to buoyancy is measured by the parameter $M_1 = \beta \chi_T^2 H_0^2 / (\rho_0 g \alpha_T (1 + \chi))$; the nonlinearity of the magnetization, $M_3 = 1 - (\chi_H H_0^2) / (1 + \chi)$, a measure of the deviation of the magnetization curve from the linear behavior $M_0 = \chi H_0$; the relative strength of the temperature dependence of the magnetic susceptibility $M_4 = \chi_T^2 H_0^2 T_0 / c_H (1 + \chi)$; and the ratio of magnetic variation of density with respect to thermal buoyancy $M_5 = \alpha_H \chi_T H_0^2 / (\alpha_T (1 + \chi))$. **(c)** (viscoelastic fluid) The Deborah number, $\Gamma = \lambda_1 \bar{\kappa} / d^2$, and the ratio between retardation and stress relaxation times, $\Lambda = \lambda_2 / \lambda_1$. Since $\lambda_{1,2}$ are positive, so are Γ and Λ . For $\Gamma = 0$ one recovers the Newtonian fluid while for $\Lambda = 0$ the Maxwellian fluid is obtained.

Let us comment on the numerical values of the parameters; the parameter Ra can be changed by several orders of magnitude, while a typical value for P in viscoelastic fluid is $P \sim 10^0 - 10^3$. The magnetic numbers have the following order of magnitude $M_1 \sim 10^{-4} - 10$, $M_3 \gtrsim 1$, $M_4 \sim M_5 \sim 10^{-6}$ for typical magnetic field strengths [29, 30]. For aqueous suspensions it is suggested that the Deborah number is about $\Gamma \sim 10^{-3} - 10^{-1}$ [56, 64, 65, 66], but for other kinds of viscoelastic fluids the Deborah number can be of the order of $\Gamma \sim 10^3$. Unfortunately, no experimental data are available for either the retardation or the stress relaxation times, so we treat Λ as arbitrary in the range $[0, 1]$. In addition, the above set of equations is still unnecessarily complicated. We will simplify it first by neglecting M_4 , which is a common simplification in the description of instabilities in ferrofluids [5]. Since M_4 is not related to viscoelastic effects, which we are interested in here, we expect not to lose any reasonable aspect of the problem under consideration. The same is true for the coefficient M_5 . So, the values of $\{M_4, M_5\}$ in the following analysis are taken to zero. Thus, we are left with two magnetic field dependent effects characterized by the parameters $\{M_1, M_3\}$. The first one denotes the influence of the Kelvin force and is expected to have the dominant influence on the convection behavior. The second parameter, M_3 is different from 1 due to the intrinsic nonlinearity of the magnetization and is only a weak function of the external magnetic field. In the next section, we study the stability of the conduction state.

3. Linear Stability Analysis

In order to calculate the linear stability, we only need the linear parts of Eqs. (13)-(17). This is readily done by neglecting the advective terms $\mathbf{v} \cdot \nabla$ and replacing D_t by ∂_t . Moreover, the effective pressure and two components of the velocity field could also easily be eliminated by applying the curl ($\nabla \times \dots$) and double curl ($\nabla \times \nabla \times \dots$) of the Navier-Stokes equation and then considering only the z-component of the resulting equations, w (i.e. the vertical velocity component). After some algebra, the linear equations read

$$P^{-1} \partial_t \nabla^2 w = \nabla^2 (\nabla \cdot \bar{\tau})_z + Ra \nabla_{\perp}^2 \mathcal{L}_{\Sigma} \quad (19)$$

$$(1 + \Gamma \partial_t) (\nabla \cdot \bar{\tau})_z = (1 + \Gamma \Lambda \partial_t) \nabla^2 w \quad (20)$$

$$\partial_t \theta = w + \nabla^2 \theta \quad (21)$$

$$(\partial_{zz} + M_3 \nabla_{\perp}^2) \phi - \partial_z \theta = 0 \quad (22)$$

where $\mathcal{L}_{\Sigma} = (1 + M_1) \theta - M_1 \partial_z \phi$. We remark that Eqs. (19) and (20) can be combined in order to get a single equation for w . One can define the vector field $\mathbf{u} = (\theta, \phi, w)^T$ that contains the important variables for the linear analysis. Using standard techniques [67], the spatial and temporal dependencies of \mathbf{u} are separated using normal mode expansion

$$\mathbf{u}(\mathbf{r}, t) = \mathbf{U}(z) \exp[i\mathbf{k} \cdot \mathbf{r}_{\perp} + st], \quad (23)$$

being $\mathbf{U} = (\Theta, \Phi, W)^T$, where \mathbf{k} is the horizontal wavenumber vector of the perturbations, \mathbf{r}_{\perp} is the horizontal vector position and where $s = \sigma + i\Omega$ denotes the complex eigenvalues; σ is the growth factor of the perturbation, and Ω its frequency. Using the ansatz (23), Eqs. (19)-(22) are reduced to the following coupled ordinary differential equations

$$D^2 \Theta = \xi_1 \Theta - W \quad (24)$$

$$D^2 \Phi = \xi_2 \Phi + D \Theta \quad (25)$$

$$D^4 W = \xi_3 D^2 W - \xi_4 W + Ra(\xi_5 \Theta - \xi_6 D \Phi) \quad (26)$$

where $D^n f = \partial_z^n f$, $\xi_1 = k^2 + \sigma$, $\xi_2 = M_3 k^2$, $\xi_3 = 2k^2 + sQ/P$, $\xi_4 = k^2(k^2 + sQ/P)$, $\xi_5 = k^2(1 + M_1)Q$ and $\xi_6 = k^2 M_1 Q$ such that $Q = (1 + s\Gamma)/(1 + s\Lambda\Gamma)$. In the following two subsections, we analyze the results of the linear stability analysis for the two considered boundary conditions.

3.1. Idealized Boundary Conditions (FF)

In order to solve the set of differential equations analytically, the following boundary conditions

$$D\Phi = \Theta = D^2 W = W = 0, \quad (27)$$

are imposed at $z = \pm 1/2$. The z-dependence of the eigenfunctions of the stability problem can then be described by simple sine and cosine functions. The eigenvalue problem produces a dispersion relation

$$\mathcal{P}(s) \equiv a_0 + a_1 s + a_2 s^2 + a_3 s^3 = 0, \quad (28)$$

where a_j are functions of the system parameters

$$a_0 = Pq^6 \varrho - k^2 P (\varrho + k^2 M_1 M_3) Ra \quad (29)$$

$$a_1 = q^4 (1 + \zeta) \varrho - k^2 \Gamma P (\varrho + k^2 M_1 M_3) Ra \quad (30)$$

$$a_2 = q^2 \varrho (1 + q^2 \Gamma [1 + P\Lambda]) \quad (31)$$

$$a_3 = q^2 \varrho \Gamma \quad (32)$$

where $\zeta = P(1 + q^2 \Gamma \Lambda)$ with $q^2 = k^2 + \pi^2$ and $\varrho = M_3 k^2 + \pi^2$. Eq. (28) allows for an analytical expression of the Rayleigh number as function of $\{s, k\}$

$$Ra = \frac{q^2 \varrho (q^2 + s) (s + \Gamma s^2 + Pq^2 \mathcal{J})}{k^2 (k^2 M_1 M_3 + \varrho) P \mathcal{T}}, \quad (33)$$

where $\mathcal{J} = 1 + s\Lambda\Gamma$ and $\mathcal{T} = 1 + s\Gamma$. There are two common particular bifurcation cases, the stationary bifurcation with $s = 0$, and the oscillatory instability that occurs when $s = i\Omega$ with Ω finite and real. For specific values of the parameters, the critical Ra values of these two instabilities, Ra_{sc} and Ra_{oc} , respectively, can be equal constituting a codimension-2 bifurcation. Let us consider first the stationary case.

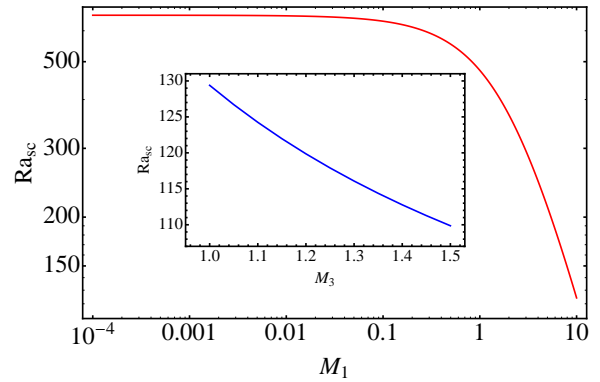


Figure 2: (Color online) Critical stationary Rayleigh number, Ra_{sc} , as a function of M_1 at $M_3 = 1.1$. The inset shows Ra_{sc} as a function of M_3 at $M_1 = 10$.

3.1.1. Stationary Bifurcation

In the stationary case ($s = 0$), we find the marginal stability curve between the Rayleigh number and the wavenumber of the perturbation

$$Ra_s = \frac{\varrho q^6}{k^2 (k^2 M_1 M_3 + \varrho)} \quad (34)$$

to be identical to that for a simple ferrofluid [22]. Hence, in this case, the viscoelastic effects do not appear at linear order. The minimum of the marginal curve (34) ($\partial_k Ra_s = 0$) gives the critical wave-number k_{sc} and, subsequently, the critical Rayleigh number, $Ra_{sc} = Ra_s(k_{sc})$, of the most unstable perturbation. Fig. 2 shows the magnetic field dependence of the linear threshold, where the field is represented by $M_1 \sim H^2$. We observe that Ra_{sc} decreases for strong fields indicating the destabilizing effect of a magnetic field. The threshold also decreases as function of M_3 (inset), although values of $M_3 > 1.5$ are rather unrealistic.

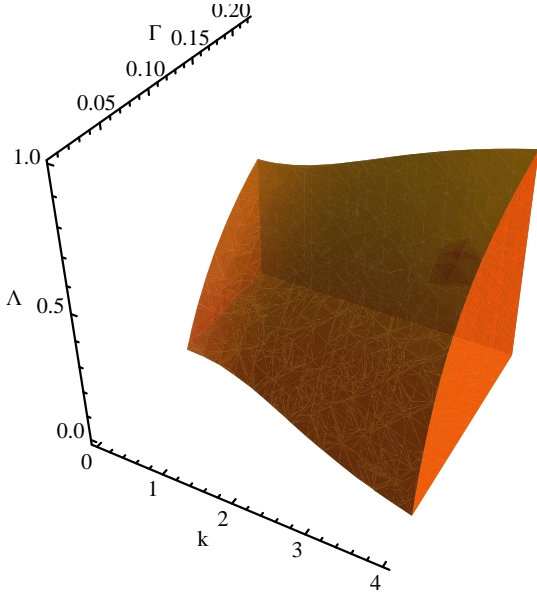


Figure 3: 3D phase diagram showing where Ω is non-vanishing as a function of the $\{k, \Gamma, \Lambda\}$ parameters.

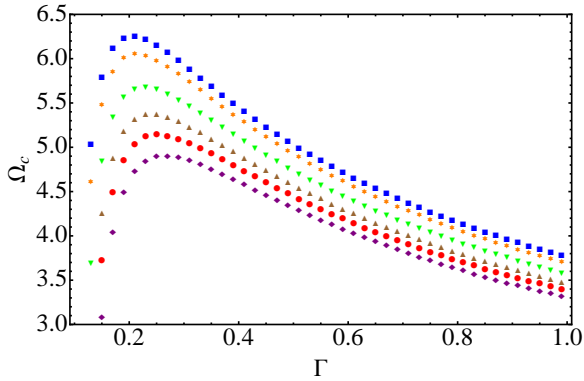


Figure 4: (Color online) Frequency of the critical perturbation, Ω_c , as a function of Γ for different values of M_1 at $P = 10$, $M_3 = 1.1$ and $\Lambda = 0.5$. The different values of M_1 are represented by different symbols from top to bottom $M_1 = \{10, 5, 2, 1, 0.5, 0.1\} = \{\blacksquare, \bullet, \blacktriangle, \blacklozenge, *\}$

3.1.2. Hopf Bifurcation

We now discuss the oscillatory bifurcation. For a nonzero real frequency Ω the eigenvalue Eq. (28) is complex and constitutes two independent conditions for its real and imaginary parts, separately. Being a cubic equation, one can easily find the two solutions $\Omega^2 = a_0/a_2$ and $\Omega^2 = a_1/a_3$, which are represented by

$$\frac{Ra_o}{Ra_s} = \Lambda + \frac{1-\Lambda}{q^4} \left(\frac{q^2}{\Gamma} - \frac{q^2}{\Gamma\Xi} + \frac{q^4}{\Xi} \right) - \frac{\Omega^2}{Pq^4} \quad (35)$$

where

$$\Omega^2 = \frac{q^2 P \Gamma (1-\Lambda) - (1+P)}{\Gamma^2 (1+P\Lambda)}, \quad (36)$$

with $\Xi = 1 + (\Gamma\Omega)^2$. For real Ω its square has to be positive. Obviously, this cannot be achieved at all for Newtonian fluids and poses a lower limit on the Deborah number for Oldroyd

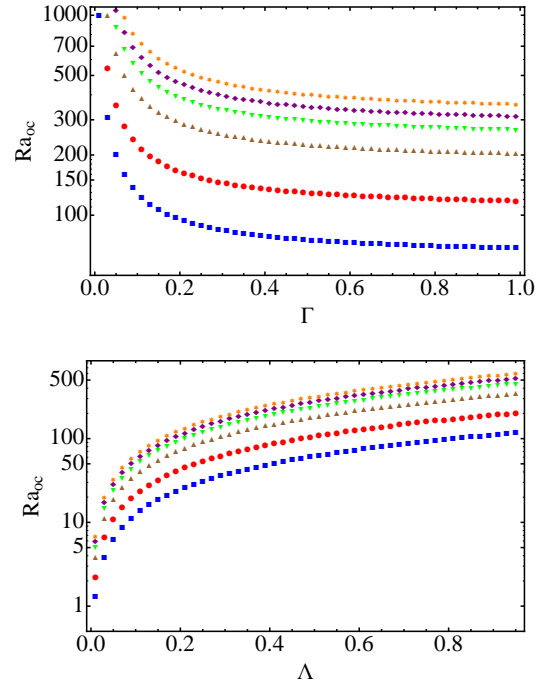


Figure 5: (Color online) Critical oscillatory Rayleigh number, Ra_{oc} , as a function of Γ (upper part) and as a function of Λ (lower part) for different values of M_1 at $P = 10$ and $M_3 = 1.1$. The different values of M_1 are represented by different symbols from bottom to top $M_1 = \{10, 5, 2, 1, 0.5, 0.1\} = \{\blacksquare, \bullet, \blacktriangle, \blacklozenge, *\}$; note the logarithmic scale of the ordinate.

(and Maxwell) fluids,

$$\Gamma \geq (1+P) / (Pq^2(1-\Lambda)) \quad (37)$$

which also means Λ must not reach the value 1. In terms of the original parameters it means that λ_1 has to exceed λ_2 by a finite, q^2 dependent amount. Note this existence condition does not depend on the magnetic field strength, although, of course, Ra_o depends on it through Ra_s . Fig. 3 shows a 3D phase diagram for the existence of oscillatory convection as a function of the parameters $\{k, \Gamma, \Lambda\}$.

The critical wave number k_{oc} follows from the condition $\partial_k Ra_o = 0$ and replacing this value in Eqs. (35) and (36) the critical Rayleigh number and frequency are obtained.

Fig. 4 shows the critical frequency, Ω_c , as a function of Deborah number, Γ , for different values of the parameter M_1 . One observes that Ω_c reaches its maximum value for intermediate values of Γ . This maximum increases when M_1 increases. Interestingly enough, one can get an approximate power law for the maximum critical frequency as a function of M_1 . It is given by the formula $\Omega_c^{max} \approx aM_1^b$ where $\{a, b\}$ are parameters that are numerically fitted. For $M_3 = 1.1$ and $P = 10$, one gets $\{a, b\} = \{5.44, 0.0628\}$. The upper part of Fig. 5 displays the critical oscillatory Rayleigh number, Ra_{oc} , as a function of the Deborah number, Γ for different values of M_1 . One observes that Ra_{oc} decreases when Γ increases and reaches an asymptotic value for $\Gamma \gg 1$. The influence of the parameter M_1 is similar to that of Γ . We have determined the asymptotic val-

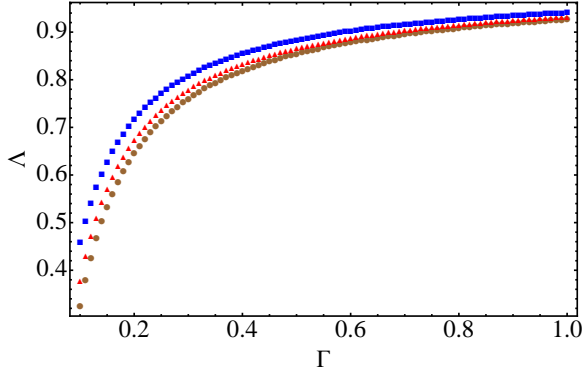


Figure 6: (Color online) The codimension-2 bifurcation line, $Ra_{sc} = Ra_{oc}$, that separates the stationary instability region (above) from the oscillatory one (below) for different values of M_1 . Parameters $P = 10$ and $M_3 = 1.1$ are held constant. The different values of M_1 are represented by different symbols, from top to bottom $M_1 = \{10, 1, 0.1\} = \{\blacksquare, \blacktriangle, \bullet\}$

ues $\Gamma \gg 1$ of Ra_{oc} in the range $M_1 \in [0, 10]$ where they follow an exponential decay law $Ra_{oc}^a = a + b \exp(-cM_1)$, with a, b, c parameters to be fitted. For $P = 10$ and $M_3 = 1.1$, one gets $\{a, b, c\} = \{60.25, 258.4, 0.359\}$. Fig. 5 (lower part) shows Ra_{oc} as a function of the ratio between the retardation and relaxation times, Λ , again for different values of M_1 . We observe that Ra_{oc} increases when Λ is increased.

We remark that the onset of the oscillatory instability (not possible for Newtonian fluids) strongly depends on the viscoelastic properties, in particular on the Deborah number. Indeed for small Deborah numbers the threshold is unrealistically high, but for large one it is drastically reduced and the oscillatory instability usually precedes the stationary instability, i.e. it occurs at a lower Rayleigh number.

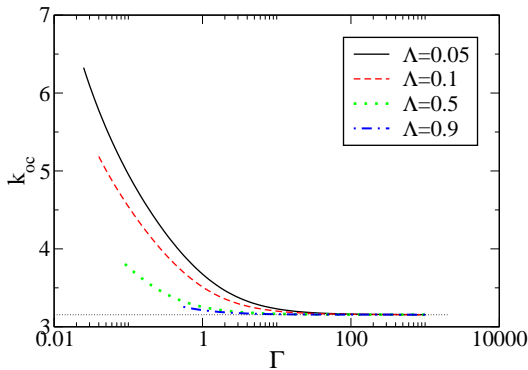


Figure 7: The critical wavenumber k_{oc} as a function of Γ for $\Lambda = 0.05$ (solid black), $= 0.1$ (dashed red), $= 0.5$ (dotted green), and $= 0.9$ (dashed-dotted blue). The horizontal dotted line indicates k_{sc} for the stationary instability. The rest of the parameters have been fixed to $P = 10$, $M_1 = 0.1$, $M_3 = 1.1$, and $\chi_b = 1$.

3.1.3. Codimension-2 Bifurcation

There exists a range of parameters where the critical oscillatory and stationary Rayleigh numbers have the same value,

$Ra_{sc} = Ra_{oc}$. This is possible due to the non-Newtonian properties of the fluid layer. Fig. 6 shows this line in the $\Gamma - \Lambda$ space that divides the stationary instability region (above) from the oscillatory one (below) for different values of M_1 . The influence of M_1 is rather weak, since Ra_{oc} has a similar M_1 dependence as Ra_{sc} . Numerically, one can fit the relationship between Γ and Λ along this line by the approximate formula

$$\Gamma = a \left[1 - \exp\left(-\frac{\Lambda}{b}\right) \right] + c\Lambda^d \quad (38)$$

where $\{a, b, c, d\}$ are fit parameters that depend on $\{P, M_3, M_1\}$. For example, if we take $P = 10$, $M_3 = 1.1$ and $M_1 = 0.1$, one gets $\{a, b, c, d\} = \{0.908, 0.17, 0.025, 5.51\}$.

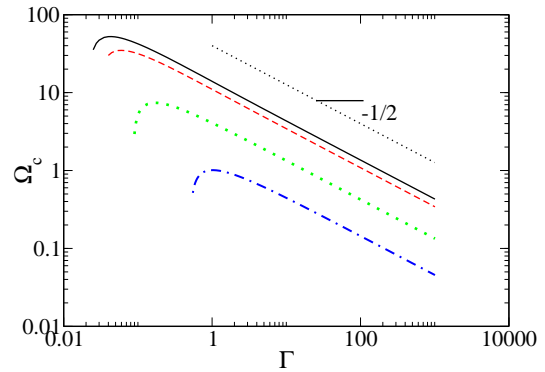


Figure 8: Same as Fig. 7 for the critical frequency Ω_c . The log-log plot reveals a slope of $-1/2$ (dotted line) for $\Gamma \gg 1$.

3.2. Realistic Boundary Conditions (RR)

The use of free-free boundary conditions at the two horizontal boundaries is a useful mathematical simplification but is not completely physically sound. The correct boundary conditions for a viscous or viscoelastic fluid is to impose

$$W = DW = \Theta = 0, \quad (39)$$

at the two horizontal rigid boundaries. In addition, in the case of a finite magnetic permeability χ_b of the rigid boundaries, the scalar magnetic potential must satisfy the following BCs

$$(1 + \chi_b)D\Phi \pm k\Phi = 0, \quad (40)$$

at $z = \pm d/2$, respectively [22]. Note that in the limit when χ_b tends to infinity, Eqs. (40) tend to $D\Phi = 0$. In order to solve Eqs. (24)-(26) with these realistic boundary conditions, we use a spectral collocation method. Spectral methods ensure an exponential convergence to the solution and are the best available numerical techniques for solving simple eigenvalue - eigenfunction problems. Here, we follow the technique of collocation points on a Chebyshev grid as described in [69]. The collocation points (Gauss-Lobato) are located at height $z_j = \cos(j\pi/N)$ where the index j runs from $j = 0$ to $j = N$.

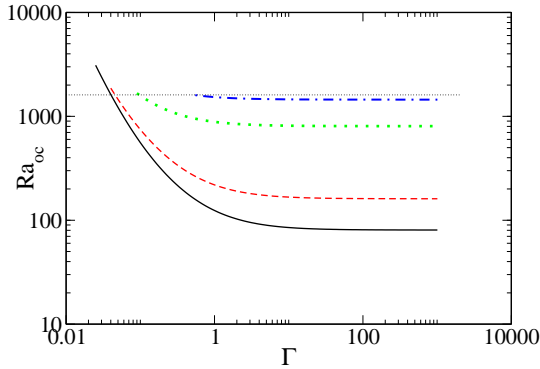


Figure 9: Same as Fig. 7 for the critical Rayleigh number Ra_{oc} . The horizontal dotted line indicates Ra_{sc} for the stationary instability.

Note that here the z -variable ranges from -1 to $+1$ and one has therefore to rescale Eqs. (24)-(26) accordingly, because the physical domain is defined in the range $(-1/2, +1/2)$.

We use $N = 8$ collocation points in the vertical direction, for which the equations and the boundary conditions are expressed. We have checked that using $N = 10$ collocation points only modifies the fourth or fifth significant digit of the result. By using the collocation method, the set of differential equations (24)-(26) is transformed into a set of linear algebraic equations. The eigenfunctions $(\Theta(z), \Phi(z), W(z))$ are transformed into eigenvectors defined at the collocation points. The Rayleigh number is again used as the eigenvalue of the problem. After this stage of discretization, one is left with a classical generalized eigenvalue–eigenvector problem that can easily be solved using the Matlab routine "eig" [70].

In the case of the oscillatory instability considered here, one has to make sure that the Rayleigh number (as being a physical quantity) is a real number by choosing a correct value for Ω . Therefore, one is left with a triplet $\{Ra, k, \Omega\}$ that defines a marginal stability condition (for a fixed value of the horizontal wavenumber k). This procedure is repeated for several values of k leading to the marginal stability curve Ra versus k . The minimum of this curve gives Ra_{oc} and k_{oc} , and the corresponding value for the critical frequency Ω_c .

Figures 7-9 show the critical quantities as functions of the viscoelastic properties of the liquid. In all three figures it is manifest that for small values of the Deborah number Γ the oscillatory instability disappears, with the threshold increasing for increasing Λ . This is in full agreement with the analytical limit, Eq. (37), obtained for idealized boundary conditions. For intermediate values of Γ , one observes in Fig. 9 the codimension-2 points, where the stationary and oscillatory convection have the same threshold. These points are shifted to higher Γ values when Λ is increased, again in agreement with the FF case (Fig. 6). For large values of the Deborah number, $\Gamma \gg 1$, the critical values show a distinctive asymptotic behavior. In particular, $k_{oc} \rightarrow k_{sc}$, the critical wavevector tends to the value of the stationary case. The oscillatory threshold $Ra_{oc} \rightarrow \Lambda Ra_{sc}$ reaches

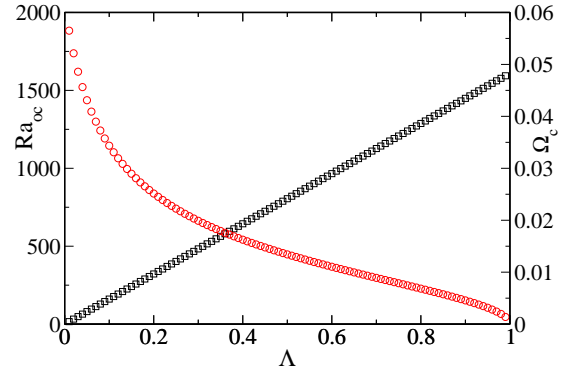


Figure 10: The critical parameters Rayleigh number Ra_{oc} (black squares) and Ω_c (red circles) as a function of Λ for a very large fixed value of the Deborah number $\Gamma = 10^5$. The other parameters are $P = 10$, $M_1 = 0.1$, $M_3 = 1.1$ and $\chi_b = 1$.

a constant value that is by the factor Λ smaller than the stationary one. This proportionality with Λ is also apparent in Fig. 10. Finally, the critical frequency goes to zero, $\Omega_c \rightarrow A/\sqrt{\Gamma}$, with an exponent of $-1/2$. The pre-factor A depends on the Deborah number. Figure 10 displays the latter dependence for a very large fixed value of $\Gamma = 10^5$ in the asymptotic regime. There is, however, no simple relation between Ω_c and Λ .

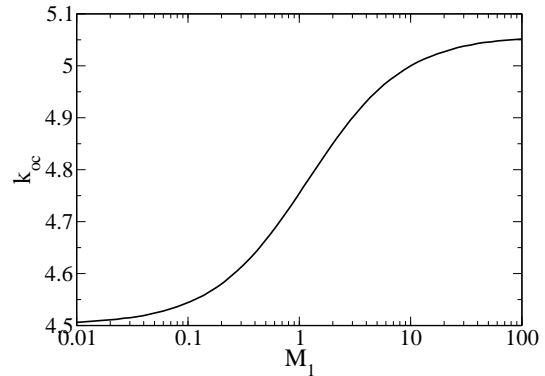


Figure 11: The critical wavevector k_{oc} as a function of $M_1 \sim H^2$ representing the external field dependence. The other parameters are $M_3 = 1.1$, $P = 10$, $\Gamma = 1$, $\Lambda = 0.1$, and $\chi_b = 1$.

For a ferrofluid an external magnetic field is an important means of manipulating its behavior. The field dependence of the critical quantities comes mainly through M_1 , which is directly proportional to the field squared, and to a much lesser extent through M_3 , which, therefore, has been kept constant for the fields considered here. In Figs. 11-13 the influence of an external field on the critical quantities is shown. k_{oc} and Ω_c increase slightly with the magnetic field. The threshold decreases rather strongly with the field and shows an asymptotic behavior $Ra_{oc} \sim 1/M_1$ for $M_1 \gg 1$. As in the stationary case, an external field is destabilizing.

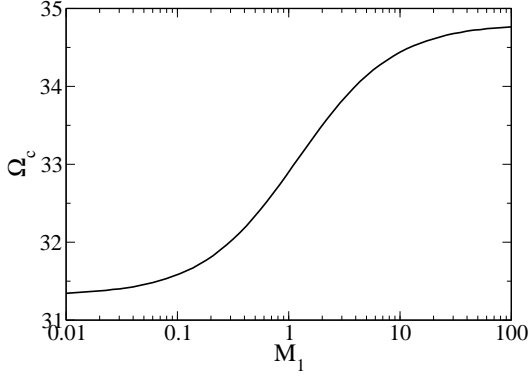


Figure 12: Same as Fig. 11 for the critical frequency Ω_c .

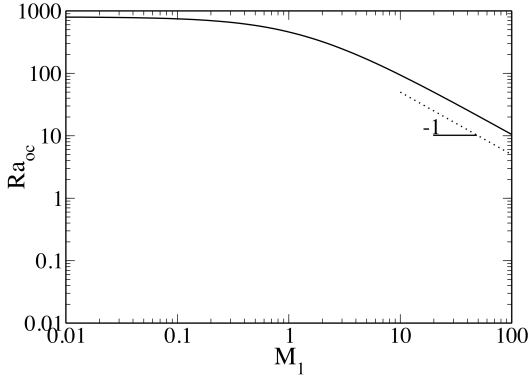


Figure 13: Same as Fig. 11 for the critical Rayleigh number Ra_{oc} . The log-log plot reveals the slope -1 (dotted line) for $M_1 \gg 1$.

We have examined the influence of the Prandtl number on the critical quantities, Ra_{oc} , Ω_c , and k_{oc} (Fig.14). While k_{oc} is rather insensitive to P , the critical frequency increases strongly, when P increases from 1 to 100. Even more interesting is the non-monotonous behavior of the threshold Ra_{oc} , which shows a minimum around $P \approx 7$. There is no simple physical explanation for this. For large Prandtl numbers the critical quantities reach asymptotically constant values. This regime is only obtained at rather high values ($P \gtrsim 200$ for the present case). This is quite different from the case of Newtonian fluids, where, as a rule of thumb, nothing changes anymore for $10 < P \rightarrow \infty$.

Finally, we show that the use of the realistic magnetic boundary conditions (40) and, in particular, a finite value of the magnetic susceptibility χ_b of the rigid boundaries does not considerably change the critical values Ra_{oc} and Ω_c as is demonstrated in Fig. 15. Both, Ra_{oc} and Ω_c , increase by only a few percent, when χ_b increases from zero to infinity, therefore justifying a posteriori the use of the simpler boundary condition $D\Phi = 0$.

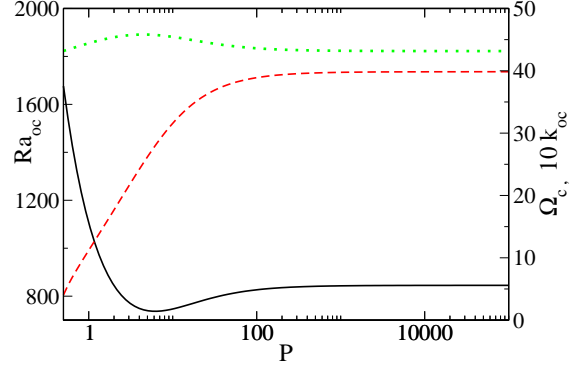


Figure 14: The critical parameters Ra_{oc} , Ω_c , and k_{oc} as a function of the Prandtl number P . The black solid line refers to Ra_{oc} (left scale), the red dashed to Ω_c and the green dotted to $10k_{oc}$ (right scale). The other parameters are fixed at $M_1 = 0.1$, $M_3 = 1.1$, $\Gamma = 0.1$, $\Lambda = 0.1$, and $\chi_b = 1$.

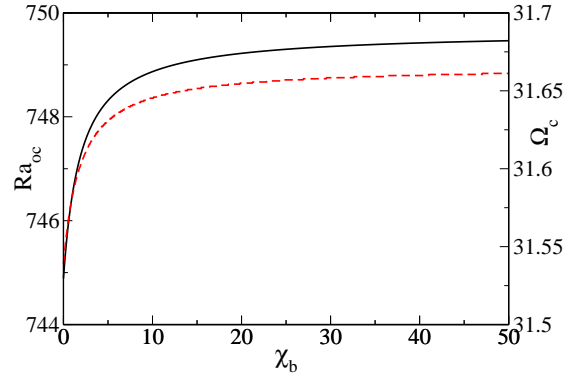


Figure 15: The critical Rayleigh number Ra_{oc} (black solid line, left scale) and Ω_c (red dashed line, right scale) as a function of the magnetic susceptibility χ_b of the rigid boundaries. The other fixed parameters are as in Fig. 14.

4. Final Remarks

In the present work, Rayleigh-Bénard convection in a magnetic viscoelastic liquid is studied. The stability thresholds for both, the stationary and the oscillatory convection, have been determined. Two different boundaries conditions for the velocity field were analyzed, the so-called free-free and rigid-rigid ones. For the former the results of Finlayson [22] for the stationary convection have been re-obtained. In addition, we have provided analytical formula for the oscillatory convection. For weakly viscoelastic fluids the critical Rayleigh number for the oscillatory convection is much higher than that for the stationary one, while for high Deborah numbers the oscillatory instability always precedes the stationary instability. In this paper, we have also calculated the range of parameters where the codimension-2 bifurcation appears. In the case of rigid-rigid boundary conditions, the convection thresholds are calculated

numerically by the spectral method. The technique of collocation points (Gauss-Lobato) as described in [69] was used.

Due to the presence of various destabilizing effects, i.e. buoyancy and magnetic forces, and of additional relaxation channels due to the Oldroyd model, the discussion of the stability curves becomes rather intricate. An oscillatory instability, whose critical frequency is a rapidly varying function of the Deborah number, is competing with the stationary one. As a result, the codimension-2 bifurcation line, separating those two instabilities, strongly depends on the structure of the Oldroyd model and its relaxation times.

Let us finally comment that, very often, ferrofluids show a finite separation ratio and a finite magnetic separation ratio and therefore require a binary mixture description. However, for materials where the separation ratio and magnetic separation ratio are not too large the simple fluid approximation is valid [29]. The present work is based on this last approximation. A detailed study on the oscillatory bifurcation for magnetic binary mixtures is still in progress.

5. Acknowledgments

D.L. acknowledges the partial financial support from FONDECYT 11080229, Millennium Scientific Initiative, P06 – 022 – F and Basal Program Center for Development of Nanoscience and Nanotechnology (CEDENNA). J.B. acknowledges financial support by MICINN (Spanish Ministry of Science and Technology) under project FIS2008-06335-C02-02.

References

- [1] B.M. Berkovsky, V.F. Medvedev and M.S. Krakov, *The Magnetic Fluids, Engineering Application*, (Oxford University Press, Oxford 1973).
- [2] M. Mahmoudi *et al.*, J. Phys. Chem. C **113**, 2322 (2009).
- [3] E. H. Kim, Y. Ahn and H. S. Lee, J. Alloys and Compounds, **434**, 633 (2007).
- [4] C. Alexiou, *et al.*, J. Drug Targeting **11**, 139 (2003).
- [5] C. Alexiou *et al.*, J. Magn. Magn. Mater. **252**, 363 (2002).
- [6] C. Alexiou, *et al.*, Cancer Research **60**, 6641 (2000).
- [7] A.S. Popel, P.C. Johnson, Ann. Rev. Fluid Mech. **37**, 43 (2005).
- [8] O.K. Baskurt, H.J. Meiselman, Sem. Throm. Hem. **29**, 435 (2003).
- [9] J.J. Bishop, Biorheology **38**, 263 (2001).
- [10] H. Shahnazian *et al.*, J. Phys. D: Appl. Phys. **42**, 205004 (2009).
- [11] D. Yu Borin, S. Odenbach, J. Phys.: Condens. Matter **21**, 246002 (2009).
- [12] S.A. Lira, J.A. Miranda, Phys. Rev. E **80**, 046313 (2009)
- [13] S.A. Lira, J.A. Miranda, Phys. Rev. E **79**, 046303 (2009)
- [14] O. Müller, D. Hahn and M. Liu, J. Phys.: Condens. Matter **18**, S2623 (2006).
- [15] P. Ilg, M. Kröger, S. Hess, Phys. Rev. E **71**, 031205 (2005).
- [16] S. Odenbach, J. Phys.: Condens. Matter **16**, R1135 (2004).
- [17] S. Odenbach, J. Phys.: Condens. Matter **15**, S1497 (2003).
- [18] H.W. Müller, M. Liu, Phys. Rev. E **64**, 061405 (2001).
- [19] B.J. de Gans, C. Blom, A.P. Philipse, J. Mellema, Phys. Rev. E **60**, 4518 (1999).
- [20] S. Odenbach, J. Mag. Mag. Mat. **201**, 149 (1999).
- [21] J.L. Neuringer and R.E. Rosensweig, Phys. Fluids **7**, 1927 (1964).
- [22] B.A. Finlayson, J. Fluid Mech. **40**, 753 (1970).
- [23] K. Gotoh and M. Yamada, J. Phys. Soc. Jpn. **51**, 3042 (1982).
- [24] P.J. Blennerhassett, F. Lin and P.J. Stiles, Proc. R. Soc. London A **433** (1991) 165.
- [25] M.D. Gupta and A.S. Gupta, Int. J. Eng. Sci. **17**, 271 (1979).
- [26] S. Venkatasubramanian and P.N. Kaloni, Int. J. Eng. Sci. **32**, 237 (1994).
- [27] P.N. Kaloni and J.X. Lou, J. Magn. Magn. Mater. **284**, 54 (2004).
- [28] G.K. Auernhammer and H.R. Brand, Eur. Phys. J. **B16**, 157 (2000).
- [29] A. Ryskin and H. Pleiner, Phys. Rev. E **69**, 046301 (2004).
- [30] D. Laroze, J. Martinez-Mardones, J. Bragard and P. Vargas, Physica A **371**, 46 (2006).
- [31] P.N. Kaloni and J.X. Lou, Phys. Rev. E **70**, 026313 (2004).
- [32] Y. Qin and P.N. Kaloni, Eur. J. Mech. B/Fluids **13**, 305 (1994).
- [33] I.S. Shivakumara, N. Rudraiah, and C.E. Nanjundappa, J. Magn. Magn. Mater. **248**, 379 (2002).
- [34] P.N. Kaloni and J.X. Lou, Phys. Rev. E **71**, 066311 (2005).
- [35] Sunil, P. Sharma, A. Mahajan, Heat. Trans. Res. **40**, 351 (2009).
- [36] Sunil, P. Chandb, P.K. Bhartia, A. Mahajan, J. Magn. Magn. Mater. **320**, 316 (2008).
- [37] S. Odenbach, Th. Volker, J. Magn. Magn. Mater. **289**, 122 (2005).
- [38] D.D. Joseph, *Fluid Dynamics of Viscoelastic Liquids* Springer, New York (1990).
- [39] C.M. Vest and A. Arpacı, J. Fluid Mech. **36**, 613 (1969).
- [40] M. Sokolov and R.I. Tanner, Phys. Fluids **15**, 534 (1972).
- [41] T. P. Lyubimova, Izv. Akad. Nauk SSSR, Mekh. Zhidk. Gaza. **2**, 181 (1974).
- [42] K.J. Röpke and P. Schümmer, Rheol. Acta **21**, 540 (1982)
- [43] J. Stastna, J. Non-Newtonian Fluid Mech. **18**, 61 (1985).
- [44] S. Rosenblat, Journal of Non-Newtonian Fluid Mech. **21**, 201 (1986).
- [45] R.W. Kolkka and G.R. Ierly, J. Non-Newtonian Fluid Mech. **25**, 299 (1987).
- [46] N. Rudraiah, P.N. Kaloni, and P.V. Radhadevi, Rheol. Acta **28**, 48 (1989).
- [47] J. Martinez-Mardones and C. Perez-Garcia, J. Phys. Condens. Matter **2**, 1981 (1990).
- [48] J. Martinez-Mardones, R. Tiemann, W. Zeller, and C. Perez-Garcia, Int. J. Bif. Chaos **4**, 1347 (1994).
- [49] J. Martinez-Mardones, R. Tiemann, and W. Zeller, Chaos, Solitons Fractal **6**, 341 (1995).
- [50] J. Martinez-Mardones, R. Tiemann, D. Walgraef and W. Zeller, Phys. Rev. E **54**, 1478 (1996).
- [51] H.M. Park, H.S. Lee, J. Non-Newtonian Fluid Mech. **60**, 1 (1995).
- [52] H.M. Park, H.S. Lee, J. Non-Newtonian Fluid Mech. **66**, 1 (1996).
- [53] P. Parmentier, G. Lebon, V. Regnier, J. Non-Newtonian Fluid Mech. **89**, 63 (2000).
- [54] P. N. Kaloni, J. X. Lou, J. Non-Newtonian Fluid Mech. **107**, 97 (2002).
- [55] P. Kolodner, J. Non-Newtonian Fluid Mech. **75**, 167 (1998).
- [56] J. Martinez-Mardones, R. Tiemann, D. Walgraef, J. Non-Newtonian Fluid Mech. **93**, 1 (2000).
- [57] J. Martinez-Mardones, R. Tiemann and D. Walgraef, Physica A **327**, 29 (2003)
- [58] D. Laroze, J. Martinez-Mardones, and C. Perez-Garcia, Int. J. Bif. Chaos **15**, 3329 (2005).
- [59] D. Laroze, J. Martinez-Mardones, J. Bragard and C. Perez-Garcia, Physica A **385**, 433 (2007).
- [60] D. Laroze, J. Martinez-Mardones, J. Bragard, Eur. Phys. J. Special Topics **146**, 291 (2007).
- [61] D. Laroze, J. Martinez-Mardones and L.M. Pérez, Int. J. Bif. Chaos **20**, 235 (2010).
- [62] D. Laroze, J. Martinez-Mardones and L.M. Pérez, R.G. Rojas, J. Magn. Magn. Mater. **322**, 3576 (2010).
- [63] T.T. Perkins, D.E. Smith, S. Chu, Science **276**, 2016 (1997).
- [64] S. R. Quake, H. Babcock, S. Chu, Nature **388**, 151 (1997).
- [65] H. Babcock, D.E. Smith, J.S. Hur, E.S.G. Shaqfeh, S. Chu, Phys. Rev. Lett. **85**, 2018 (2000).
- [66] S. Chandrasekhar, *Hydrodynamic and Hydromagnetic Stability*, Dover, New-York (1981).
- [67] H. Pleiner, M. Liu and H.R. Brand, Rheologica Acta. **43**, 502 (2004).
- [68] L.N. Trefethen, *Spectral Methods in Matlab*, SIAM, Philadelphia (2000).
- [69] Matlab7 from Mathworks Inc., Natick, MA (USA).